

The Frasnian, Central Iran: biostratigraphy, facies analysis, paleoenvironment and sea level changes

Ava Alizadeh¹, Afshin Hashmie^{2*}, and Neda Ghotbi³

¹Department of Geology, Faculty of Earth Science, Azad University, Tehran, Iran.

²Independent researcher, Graduated from Sedimentology, Shiraz, Iran.

³Department of Geology, Faculty of Earth Sciences, Shiraz University, Shiraz, Iran.

*Corresponding author's email: hashmieafshin@gmail.com

Submitted date: 21/03/2020 Accepted date: 24/02/2021 Published online: 31/03/2021

Abstract

Two section in Bahram Formation for biostratigraphy, lithofacies, facies, paleoenvironment and sequence stratigraphy were studied. In this article to with the sequence stratigraphy of the Upper Devonian (Frasnian) Bahram Formation for this reason micro/lithofacies analysis of the sediments in the south toward northeastward part of the main Iran plate Mountains. According to stratigraphic distribution Bahram Formation at the study sections is of Frasnian stage, based on the occurrence of Umbrella algae species in Shaftalugaltan section and conodonts in Sar-e-Ashk section. The main bioclastic components of the Bahram Formation are brachiopods, algae, bryozoans, corals, gastropods and fragment fossil. Microscopic investigation confirms the presence of eleven petro/microfacies typical for upward shallowing trend from in five micro/lithofacies belts shallow-open marine to shoal, restricted lagoon, and toward tidal flat and finally to near-shore depositional environments were identified. According to the evidence of environmental interpretations, we reconstructed a mix carbonate-siliciclastic shallow-water shelf mainly represented by its middle and inner sectors. The vertical expansion of the investigated litho/petro/microfacies provide for 3rd-order cyclic in the Bahram Formation. Comparison of the recommended sedimentary sequences with those reported in Iranian plate and the local relational change sea-level curves related, well with the worldwide change sea-level curves.

Keywords: Central Iran, Frasnian, Paleoenvironments, Sequence stratigraphy.

1. Introduction

The Bahram Formation is part of a Devonian rocks that forms by the sedimentary cover of the Pan-African cratonic basement (Sharland et al. 2001). The study region during the Devonian were annexed to the African and Arabian plates and constructed of the cratonic Gondwana and of the Paleo-Tethys (Blant 1978; Al-Juboury and Al- Hadidy 2009). The Bahram Formation, of Givetian to Famennian age (Wendt et al. 2005; Gholamalian et al. 2003, 2007, 2008, 2009; Bahrami et al. 2011, 2014), have rich fossil debris (Abundance of brachiopods) in Central Iran. The Bahram Formation was named concerning the Ozbak Kuh in Sartakht Bahram area (north of Tabas Block) by Ruttner et al. (1968). According to Aghanabati (2004), Bahram Formation is in lower part of the Ozbak kuh group (Fig. 1). Lithostratigraphically, the Bahram Formation, on the type section, be composed of principally limestones with abundant brachiopods and intercalation of dolomitic limestone, shale and

marl (Aghanabati 2004). The Middle-Late Devonian rocks in structural units of Iran are Muli and Zakeen formations in Zagros and Khoshyilagh Formation in Alborz Iran (Fig. 2). General studies to identify of the Bahram Formation are due to Flugel and Ruttner (1962), Ruttner et al. (1968), Later, this Formation studied by Stockline et al. (1965) to review and recuperate the previous works and explain the Bahram Formation throughout the Central Iran basin (Dastanpour and Bassett 1998). Recently biostratigraphy (by studying conodonts, Palynological and brachiopods) of this Formation was studied by Morzadec et al. (2002), Ghavidel-syooki and Mahdavian (2010), Gholamalian (2003, and 2007), Gholamalian and Kebriaei (2008), Gholamalian et al. (2009), Bahrami et al. (2011, and 2014), Webster et al. (2003), Wendt et al. (1997, 2002 and 2005). The palaeobiogeographic and paleoenvironmental studies of this Formation were directed by Wendt et al., (1997, 2002, 2005), Khosravi et al., (2014), Hashmie et al., (2015 and 2016), Hoseinabadi et al.,

(2015), Mistiaen et al., (2015). Since there are not any studies on the biostratigraphy in Shaftalu-ghaltn section), paleoenvironments and change sea levels of the Bahram Formation in the both section outcrop or the connected reports are not available. Since the goal of this study is to describe and explain the lithostratigraphy, biostratigraphy petro/microfacies and depositional environment applying both field and petrographic observations. Finally, based on biostratigraphy and petro/microfacies change we examine the change sea leveling of this Formation in Shaftalugaltan and Sar-e-Ashk sections and correlate with other sections.

2. Geological background and study area

Tectonic events and sedimentary rock in Iran resulted several explainable structural and sedimentary regions. Iran plate is located within the active convergence intermediate to the Eurasian and Arabian plates (Locombe and Mouthereau, 2006). During the Palaeozoic, Arabian plate together with Iran Plate (Fig.2), India and Afghanistan, invented the long, very broad and fixed passive margin of Gondwanaland abutting the Middle-Eastern Paleo-Tethys toward north (Sepehr and Cosgrove 2004). The geology history of the area may be summarized as follows: The Paleozoic to Middle Triassic formation were folded in pre-Upper Triassic time (Early Cimmerian orogenic phase) probably with an accompanying metamorphism (Eftekhar Nezhad et al. 1983). The palaeotectonic position indicates that enormous portions of the northern Gondwana margin in Iran must have been subducted during the continent convergence and elimination of the Palaeotethys Ocean (Eftekhar Nezhad et al 1983). Bozorgnia, (1964) also reported Givetian or Frasnian tentaculitid limestones from approximately the same area. The Devonian sequence exposed in a Shaftalugaltan and Sar-e-Ashk sections proved to be a several hundred meters wide thrust zone in which tectonically imbricated wedges of Triassic? Dolomites and Devonian bed occur. The occurrence of typical Devonian platform deposits in this area, similar to those on the Central-East-Iran Microplate, is noteworthy (Wendt et al. 2005). In contrast in

Shaftalughltan section, the Palaeozoic core of the mountain ranges SW of Torbat-e-Jam consists of unmetamorphosed rocks which constitute the northeastern margin of the platform deposits in Iran, outside the Central-East-Iran Microplate (Wendt et al. 2005). This pile is thrust over Neogene sediments, with a thin wedge of Bahram Formation at the base of the thrust plane. In Central Iran zone, rocks of all ages are present, from Precambrian to Quaternary, and, magmatism, several episodes of orogeny and metamorphism can be identified. Precambrian to Cretaceous rocks are exposed in the Shaftalugaltan and Sar-e-Ashk sections (Fig.3 c and d). The older Devonian unit in this area is the Padeha Formation, constituted by sandstones and siltstone with intercalated and conglomerates and dolomites that deposition in a very shallow sea shelf. In Sar-e-Ashk section Padeha Formation is overlaid by the Sizbar Formation (dolomitic unit) that deposited very shallow subtidal to supratidal environment (Bahrami et al., 2014). This Formation conformably overlies of the Sibzar Formation in Shaftalugaltan section, Padeha Formation in Sar-e-Ashk section and Bahram Formation unconformably overlies by dolomitic Shotori Formation (Triassic) in Shaftalugaltan section and by Jamal Formation in Sar-e-Ashk section respectively (Fig.3 c and d).

3. Methods

This study consists of field and laboratory examination of the Bahram Formation in two different stratigraphic sections (Shaftalugaltan section, 45 km along the Torbat-e-jam-Bakharz road, toward Baei village; and Sar-e-Ashk section, 72 km northeast of Kerman city along the Horjend-Ravar road) of the Central Iran (Fig. 3a and b). Facies types and their paleoenvironments were decided based on the field studied and petro/microfacies criteria and comparison with paleoenvironments (Wilson 1975; Flugel 2010). Facies explanation was based on the, fossil content, texture, grain size, and grain composition (Flugel 2010). More than 150 sample were collected in field for petrographic studies. Thin sections were studied with the Polarized microscope for facies analysis, biostratigraphy and sequence stratigraphy. Carbonate facies are ordered on

| System and stage | Model | Egypt | Saudi Arabia | Iraq Khabour | Iran Tabas Alborz Maku | Turkey Hazro and Hakkari Bythinia Toros |
|------------------|------------------------|---------|--------------|----------------------------|----------------------------|---|
| Carboniferous | | Desouqy | Berwath | Harur | Sardar Mobarak | Kapulu Baltaman Kerucuk |
| Famennian | Hercynian Orogeny | | | Ora | | |
| Frasnian | | | Juban | Kajsta | Shishu Geirud Khoshyeilagh | Akdare |
| Givetian | | | | Pirispiki Chalki volcanics | Bahram | Dadas |
| Emsian | Devonian Transgression | Zeitoun | | | Jamal | Yeginli |
| Sigenian | | Jauf | | | Muli | Pendlk Buyukada |
| Gedinnian | | | Tawil | | Sibzar | |
| | | | | Padeha | | Sigireik |
| | | | | | | Akviran Karayar |

Fig. 2. Devonian strata of Iran, Iraq, Saudi Arabia, Egypt and Turkey (with slightly modified after Hussein, 1991).

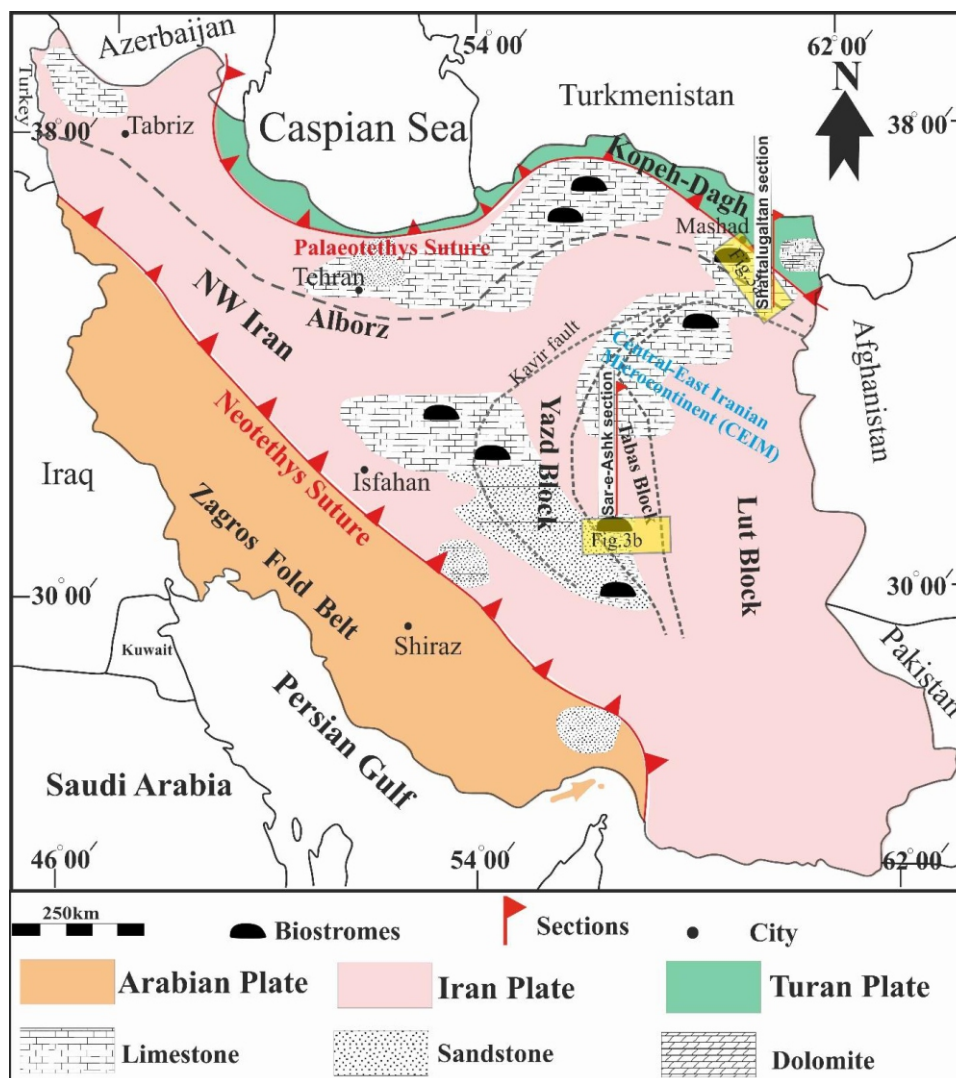


Fig. 2. Location map of the study area and measured stratigraphic section in the Plate Iran Basin Sketch map of Iran showing the inner micro blocks. Map of present-day of Iran showing the geographical domains as well as the lithology pattern and palaeogeography of the Upper Devonian (Bahram Formation) and the main sutures and tectonic structures (modified from Wilmsen et al. 2010 and Wendt et al. 2005); moreover, a close-up view of square of the study area (Fig.3).

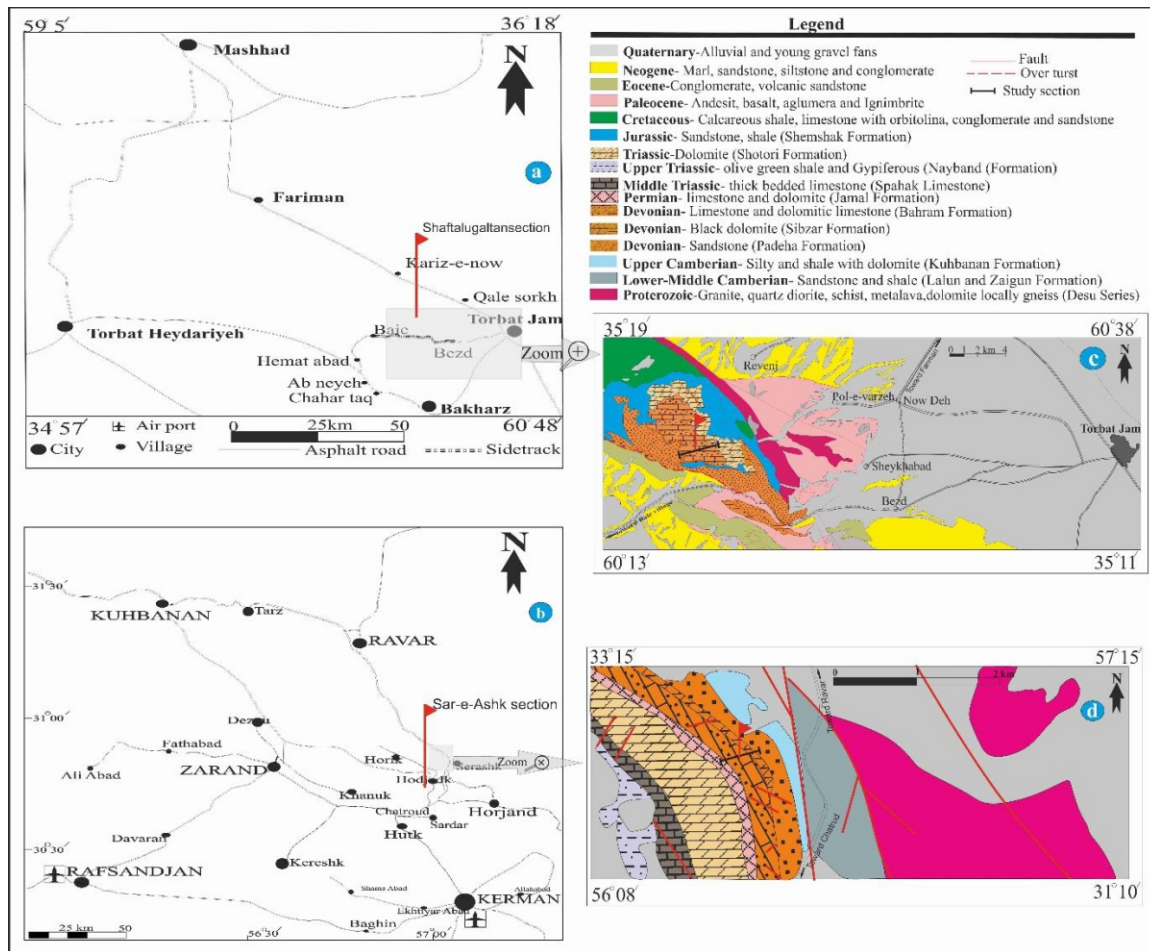


Fig. 3. (a) Location of the study area at Shaftalugaltan section in north of Central Iran. (b) Locations of measured Sar-e-Ashk section in south Central Iran (c and d) Schematic geological map of study area based on age of sediments (Eftekhar Nezhad et al. 1983 and Alavi et al. 1996) at the Saftalugaltan section. (d) Simplified geological maps of the Sar-e-Ashk section with locations of the studied section (Vahdati-Daneshmand et al. (1995)). Position of study section with detailed distribution of formations.

the basis of Dunham (1962) and Embry and Klovan (1971) textural classification scheme. The petro/lithofacies descriptive statement follows Pettijohn et al. (1987) and Miall (2006). The mud limestone description classified the scheme of Dorrik (2010). Biostratigraphy is determined based on the well-known Umbrella species of Bozorgnia (1973) Bykova (1955) and Madler (1957). For sequence stratigraphic analysis the standard models defined by Emery and Myers (1996), Catuneanu, (2006, and 2019) and Catuneanu et al. (2009) were followed and were correlated with other study in central Iran.

4. Lithostratigraphy in Shaftalugaltan section

This section is named after its exposure at the north of Baei village of Bakharz city. The

study area (Shaftalu-galtan Mountain) is located in the northeast Central Iran basin. Bahram Formation in Shaftalugaltan is 131 m thick and chiefly contented of thin to very thick bedded limestone with intercalation and alternative beds of dololimestone, sandstone and shale in the lower and upper part and thin to thick bedded limestone in the middle part. The stratigraphic succession from the Bahram Formations is shown in Fig.4. According to observation in the field, we divided Bahram Formation into five lithological unit's stratigraphy. Unit 1 with a thickness of 40 m be composed alternation of medium to very thick-bedded or gray limestone and sandy limestone (Fig.6 f) with dark gray, thick bedded dolomite and olive green silty shale and mudstone (Fig.6 a). Unit2 (4 m), brown color, fine to medium grain, with cross-bedding and laminatoin with medium to thick bedded. Unit3, with a

thickness of 35 m is composed of light gray medium to thick bedded limestone (Fig. 8a). Common fossil component are calcareous algae, brachiopods, crinoid, coral, bryozoan and mollusks (Fig. 7 k and l). The upper limestone generally seems thin to medium bedded and fine to coarse grained with a grainstone texture. Unit 4, thick bedded, grey to light grey, fine to coarse grain, contain ripple mark, cross-bedding (Fig. 6d) and with a thickness of 13m. Unit 5, with a 21 m thickness is composed alternation of light gray to cream color, medium-bedded dolomite and limestone and is abundance in ooids and sandy limestone having lamination and intercalation of gray shale, silty shale and dark gray medium bed dolomite (Fig. 7e). Fossil constituents are fossil debris and bivalves. In the upper part of unit is sandstone (4m), which is coarse grained, white and medium bedded overlain by light cream dolomite of the Dolomite Shotori Formation (Fig. 4). Bahram Formation overlies conformably the Sibzar Formation in this section and samples from Sibzar and Shotori Formation have been studied.

5. Lithostratigraphy in Sar-e-Ashk section

The Sar-e-Ashk section is located on the northern flank of the Hojedk synclinal, just north of the Sar-e-Ashk village (Fig. 3 b). In this section, this formation is overlies by the Padeha Formation. The thickness of Bahram Formation is 251 m, which gradually changes to Jamal Formation the lithology of this Formation in this section consists mainly of sandstones, calcareous sand, limestone, shale and siltstone (Fig. 5). The base of the section is marked by a northwest southeast trending fault that causes contiguity of the Middle-Upper Cambrian Kuhbanan Formation with the Padeha Formation of probable Givetian. (Bahrami et al., 2014). The Bahram Formation in this section be composed of an alternating strata of five consecutive units ordered from base to top; Unit 1 is consisting of (80m) gray to brown sandy-limestone and siltstone with intercalation of thin to medium, grey, thick limestone, contain debris fossil with intercalation of dolomite and shale form (siltstone); Unit 2 is brown, fine grain, sandstone, contain of cross-bedding and lamination (17m). Unit stratigraphy 3 with a

38m thickness that consists of light gray medium to thick bedded limestone, highly fossiliferous (brachiopods, rugose, tabulate, corals, bryozoan, and tentaculitids) (biostromal limestones) with intercalation of shale and dolomitic limestone. Unit 3 composed (37m) alternative gray, medium to thick bedded sandy-limestone and limestone with thin intercalations of shale, brachiopods debris. Unit 4, grey to brown, fine to coarse grain, thick bedded sandstone, contain of cross-bedding with 25m thickness. Base on field studies, the upper and lower link of the unit 3 possibly easily respected by the full range of brachiopods debris. Unit 5) 89 meter of gray to dark limestones, fossiliferous (brachiopoda, bivalves, crinoids, gastropods and calcareous algae) with intercalation of grey to green shale and marl.

6. Biostratigraphy of Shaftalugaltan section

The Frasnian-Famennian extinguishment event is known to have infected many groups of ocean organisms (Copper 2002). A detailed age for Sibzar dolomite Formation interval cannot be achieved. Therefore, based on this stratigraphic position, the interval is dated Late Devonian age. Shotori Formation is unconformably top by the Bahram Formation and the fossils of this formation is dated as Carboniferous-Middle Triassic. The microfossils and Umbrella zone of Bahram Formation are: Umbrella rotundata, Umbrella shahrudensis, Umbrella sp., ostracods, brachiopods, bivalves, shell fragments, worm tubes, bryozoans, corals, gastropods, crinoids and echinoids (Fig. 4). In the study section conodont fauna is very sparse in these samples; only a few of them contain conodont elements. Conodonts recovery from this interval was poor indicating only a general upper Devonian. A conodont sample from the last has yielded an early Frasnian (rhenana Zone) (Fig. 4). The appearance of Umbrella shahrudensis and Umbrella rotundata this part is indicating the Umbrella zone of Bozorgnia, 1973 are marked the Frasnian (Late Devonian). Bozorgnia, (1973) established a biostratigraphic zonation for the Devonian units in Iran. Umbrella zone have been recognized, allowing to assign the Bahram Formation of this section to the Frasnian (Figs. 4).

7. Biostratigraphy of Sar-e-Ashk section

The conodont fauna assembles in Sar-e-Ashk section enable to apportion a Frasnian to the Bahram Formation (Bahrami et al., 2014). The Bahram Formation in Sar-e-Ashk section is marked as lower falsiovalis-upper marginifera zones (Frasnian). Two Lower falsiovalis Zone to the linguiformis zones are erected (Figs. 5).

8. Facies analysis and paleoenvironmental interpretation

These major facies and sub-facies described and interpreted below, and summarized in Figures 4 and 5. Based on sedimentological characterize and skeletal and nonskeletal ingredient, 11 microfacies are recognized. These facies are connected to the five depositional belts of inner and middle portions of a shelf. In the following, each petro/microfacies is described and interpreted.

9. Clastic-dominated facies

The studied strata are subdivided into different lithofacies or petro-/microfacies. Each one is characterized by dominating skeletal, non-skeletal components and sedimentary structures. Based on the palaeoenvironmental and sedimentological analysis, detrital facies (foreshore, shoreface, and offshore) belts can be recognized.

9.1. Quartz arenite petrofacies

Field observations

The roundness of grains and the maturity of sandstones increase from the brown bed to light red to pale brown sandstones. This petrofacies described the upper beds of unit 2 and 4 rock of the Bahram Formation in both sections, with a thickness apparently ranging from 0.5 to 2 m. It is principally contain of st and sp, lithofacies (Miall 2006) that is, in parts, rich in quartz grains. These petrofacies are composed of medium to coarse-grained sandstones that have been observed only. This facies is particular of trough cross-bed, planar cross-bedding with herringbone and ripples with complex crests (Fig. 6 a, b, c and d).

Description of Petrofacies

The quartz grains are nearly exclusively monocrystalline and there are also several microgranular polycrystalline quartz grains (Fig. 6 e). Most quartz grains have very many inclusions and a small number quartz grains show euhedral texture (Fig. 6 e). The Quartz overgrowths as small crystals observed in the facies which shows the amount of coagulation variable towards full coverage of quartz grains.

Interpretation

Quartz arenite petrofacies of the Bahram Formation in study area lack typical shore sedimentary properties produced by marine activities at high energy. Because of these, sandstone facies are usually poorly classified and this indicates that they are not transported and reworked and can be interpreted as shoreface deposits. A similar facies type is delineated by Hashmie et al. (2015) and Wendt et al. (2002). Poorly grow together quartz overgrowths are the upper shoreface and foreshore, whereas St and Sp lithofacies are usual in the lower shoreface (Khalifa and Morad 2015). Clastic deposits with characterize such as herringbone cross-bedding, ripple marks and trough and planar cross-bedding in lithofacies in organization with mature, fine-crystalline dolomitic limestone display that they have deposited in a coastal or tidal flat belt (Siddiqui et al. 2017). The planar cross-lamination and trough cross-lamination sandstones indicate deposition above the fair-weather indicates a suitable climate in a high-energy coastal environment (Reading 2009).

9.2. Quartz wacke petrofacies

Field observations

This petrofacies was observed in most unit1 in Sar-e-Ashk section and in the unit 2 of Shaftalugaltan section. This petrofacies is observed in olive green to grey colors (Fig. 6f) that alternates with Quartz arenite petrofacies. This is sr and sh lithofacies and facies shale form and wacke are frequently intercalated in sandstone layers. Sedimentary structures such as ripple marks with straight, sinusoidal,

bifurcate, and complex crest lines that are symmetric can be seen in this lithofacies. The main characteristic of these lithofacies is the existence of different shapes of wavy ripple marks with sinusoidal and symmetrical. Basal

erosion surfaces are similar to the trough and planar cross-beds, and both substrates are displayed in reverse and inverted degrees (Fig. 6d).

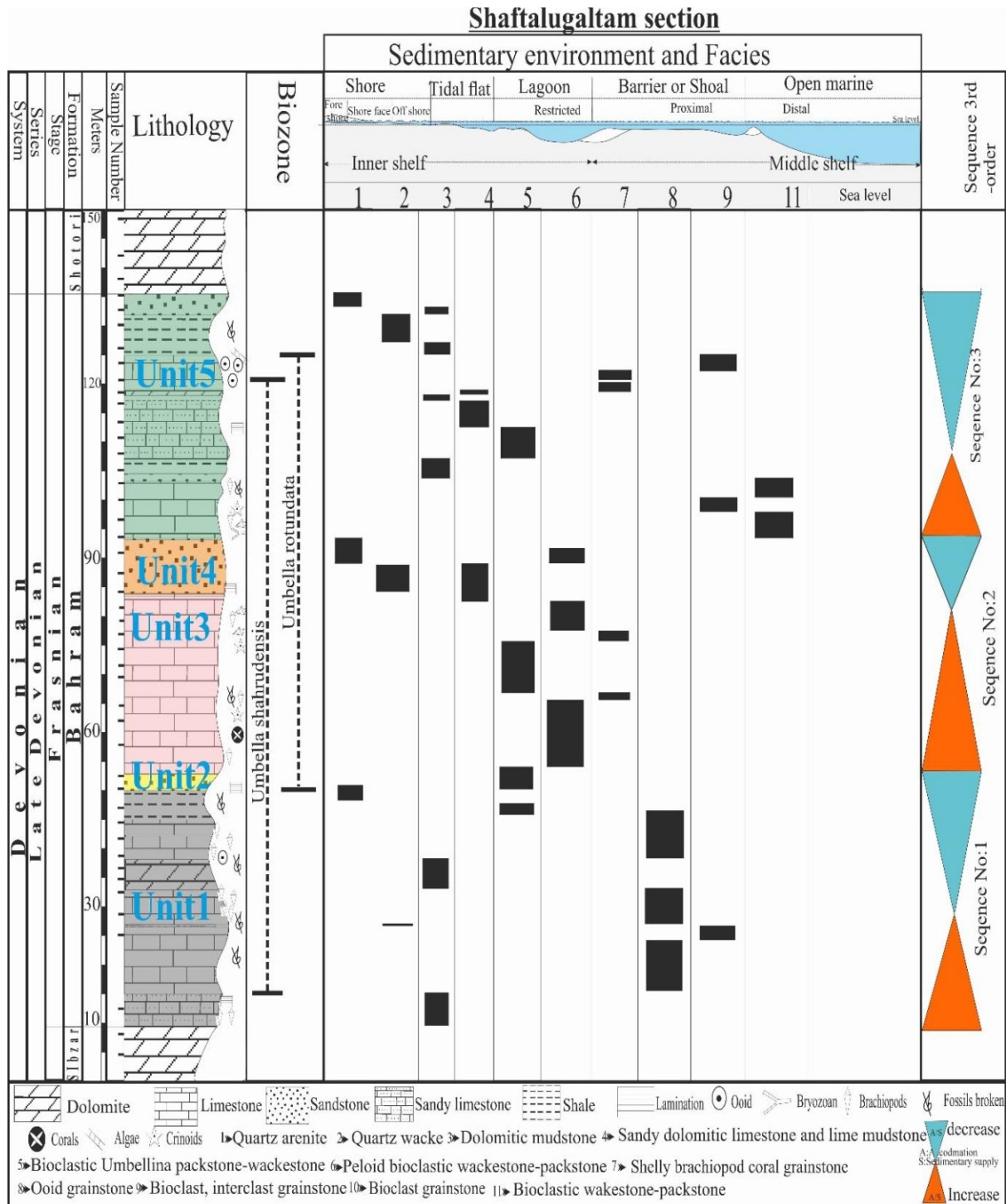


Fig. 4. Lithology, biostratigraphy, paleo-environment column, sequence stratigraphy and abundance, range of allochem, vertical distribution of microfacies, and interpreted water depth Bahram Formation at Shaftalugaltan section.

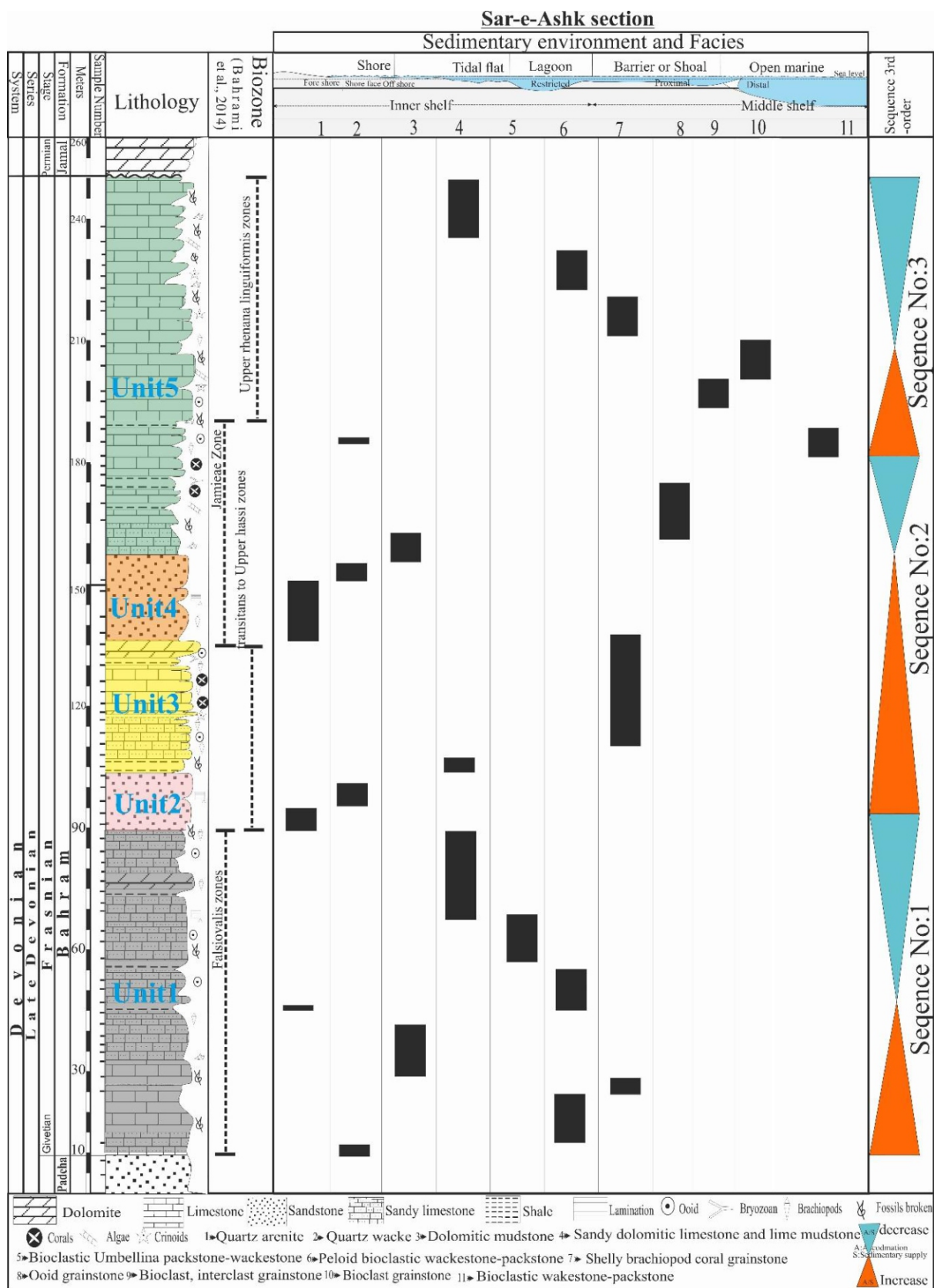


Fig. 5. Vertical facies distribution, biostratigraphy, paleo-environment column and sequences stratigraphy of the Bahram Formation in Sar-e-Ashk section.

Description of Petrofacies

This petrofacies consists of Mono/polycrystalline quartz grains, feldspar, micritic limestone and subordinate mica. The grains are subrounded to rounded, moderately sorted and cemented by dolomite and micritic calcite in some samples and iron oxides (Fig. 6g and h). Carbonate grains are up to 2.5 mm in size, whereas are angular and so are also many feldspar grains broken along their cleavage planes. Strata have a vertical upward trend, and sometimes they show a planar stratification.

Interpretation

The grain size is in extend of sand grain, but in some places it contains silt and mud. Rock fragments, plagioclase and mica are present with 10% low percentage and exhibit moderate sorting and grains are angular–subangular (Fig. 6h). During low water flow, horizontal layers form on the facies. This petrofacies relationship is related to continuous changes in environmental energy and based on these energy changes, medium quartz and wacke are formed. Increasing the energy level for a longer period of time leads to the deposition of coarse grain sandstone lithofacies on sediments very small size.

10. Carbonate-clastic dominated facies

10.1. Dolomitic mudstone microfacies

Field observations

The dolomitic microfacies, which is generally yellowish is not poriferous. This microfacies is homogeneous, unfossiliferous dolomitic mudstones, fine grained dolomite comprising dolomitic lime-mudstone and dolomite microfacies.

Description of microfacies

The matrix of this microfacies is composed mainly of lime-mud. There is also a small percentage of quartz grains (Fig. 6 i and j). The matrix is characterized by an abundance of fine-grained dolomite crystals with no fossils.

Interpretation

This is microfacies formed very shallow,

low-energy configurations near the shore at the flat tide. Due to the lack of fine-grained crystals, the lack of fossils, the presence of quartz grains the size of mud (Mahboubi et al. 2001, Flügel 2010). Where the sediment is completely dolomite, the rhombic shape of the dolomite crystals may no longer be pretended in the thin section. These dolomites are almost identical to those registered by many researchers in archaic tidal flats (Khalifa 1982). Some workers believe that dolomitic lime-mudstone is formed during early diagenesis in super/intertidal (Gregg and Shelton 1990). This microfacies is comparable to SMF 25 of Wilson (1975) and RMF 22 of Flügel (2010).

10.2. Sandy dolomitic limestone and lime mudstone microfacies

Field observations

This is microfacies characterised by thin to medium bedded and light grey and it includes bioclastic dolomite and fabric-destructive dolomite in macroscopic sedimentary structure. In this microfacies by homogenous lime mudstone, non-laminated, a little debris fossil and very fine to coarse-sized quartz grains are scattered within the matrix are present.

Description of petrofacies

Dolomicrite microfacies extensive in size from 20 to 70 mm, contains inflated quartz grains the size of silt (Fig. 6k).

Interpretation

Mud texture, quartz grain, fossil debris, dolomitic and the lack of subaerial exposure characteristics in these microfacies are sedimentary environmental indicators of the lower part of the inter-tidal setting. The presence of scattered sparry cement and fossil debris in some parts of the microfacies indicates that these are affected by tidal currents near the shoal in a medium to high energy environment. In accord with Flügel (2010), deposits consisting of a mixture of carbonate and elastic silicate materials are shared in indoor shelf settings. This microfacies is comparable to SMF 25 of Wilson (1975) and RMF 25 of Flügel (2010).



Fig. 6. Field photos and microscope photo show characteristics of identified lithology and contain allochem in the Bahram Formation. (a) Succession quartzarenite and Quartz wacke with Lamination and planar cross-bedding. (b and c) Beds of horizontal and laminated and planar cross-bedding in st and sp lithofacies and quartzarenite petrofacies. (d) Symmetrical ripple mark in Quartz wacke petrofacies in Sar-e-ashk section. (e) quartzarenite petrofacies with quartz grain. (f) Succession alternation shale and limestone. (g) Sandy dolomitic lime mudstone microfacies. (h) Sandy dolomitic limestone and lime mudstone microfacies. (i) Dolomitic mudstone microfacies (arrows) quartz grain. (j) Subhedral dolomitic crystal in dolomitic mudstone microfacies (k) Sandy dolomitic limestone microfacies in Saftalugaltan section. All photos are taken under XPL light.



Fig. 7. Photomicrographs of the some selected *Umbellina* alga. (a and b) Limestone (packstone) with *Umbella rotunda*, *Umbella* sp and fossil debris (arrows) upper picture, PPL. (c and d) Limestone (packstone) with *Umbella shahrudensis* and fossil debris, PPL. (e) Alternation of dolomitic mudstone, quartz wacke and limestone in Sar-e-ashk section. (f) Bioclastic *Umbellina* packstone-wackestone microfacies. (g) Peloid bioclastic wackestone-packstone microfacies. (h) Bioclastic intraclast grainstone microfacies. (i, j and k) coral fossil in shaly brachiopod coral grain stone in Sar-e-Ashk section. (l) Shelly brachiopod coral grainstone microfacies in Shaftalugaltan section with bryozan (arrows red), coral (arrows blue) and Brachiopods (arrows green).

11. Carbonate dominated facies

11.1. Bioclastic *Umbellina* packstone-wackestone microfacies

Field observations

This microfacies, comprising up to 40% of the unit 1, 3 and 5, was most usually recorded in unit 3 of both sections, with a thickness determined from 1 to 2.5 m. It is composed of intermittent limestones with medium-sized marl limestone beds that had a light olive green to light gray, hard, thin bedding and contained the remains of brachiopods, corals and echinoids, and two very rare valves. No evidence of widespread diagenesis and outstanding porosity in this area has been identified.

Description of microfacies

The main component in this microfacies is *Umbellina* (Fig. 7a, b, c and d). *Umbellina* rotundata, *Umbellina* shahrudensis, *Umbellina* sp., and fragment brachiopods, coral, crinoids, gastropod, and bivalves are very rare the common skeletal components (Figs. 7i and 8a). This is a facies with algae, with packstone-wackestone texture, displaying lagoon paleoenvironment (Husinec and Sokac 2006).

Interpretation

A restricted lagoon environment is recommended for this microfacies. Restricted conditions are proposed abundant skeletal components of living organisms and with low energy (Geel 2000). The abundance of *Umbellina* species are commonly considered as evidence for restricted lagoon environments (Stewart Edgell 2003). The abundance of *Umbellina* species is usually recognized as a document for relatively rocky and / or comparison nutrient-rich back-reef belt (Stewart Edgell 2003). This microfacies is analogous to SMF 18 of Wilson (1975) and RMF 20 of Flügel (2010).

11.2. Peloidal bioclastic wackestone-packstone microfacies

Field observations

This microfacies is medium bedded with

clastic grains. This microfacies is dominated with coarse-grained poorly sorted packstone-wackestone and consists of light grey medium beds mainly composed of fossil debris and peloids with 40% abundance and uniform in size.

Description of microfacies

This is a facies represented by an association of peloids with a median size of 0.4 mm (Fig. 7 f, g and h). Pieces of bivalve and green algae with a predominant texture supported by flowers.

Interpretation

Sedimentological data and plenty of peloids in this microfacies show that sedimentation happened in a restricted lagoonal belt with a weak link with the shallow open-marine and below the FWFB, with low-energy background conditions (Wanas 2008, Tomasovych 2004). The lime-mud controlled sequence and stratigraphic position attendance, of bioclast indicate that deposition took place in a low energy. This microfacies is analogous to SMF 16 of Wilson (1975) and RMF 4 of Flügel (2010).

11.3. Shelly brachiopod coral grainstone

Field observations

This microfacies characterizes unit 1 and 3 rock of the Bahram Formation in both sections, with a thickness apparently ranging from 0.2 to 0.4 m. It is principally composed of marly limestone, a limestone that is, in parts, rich in brachiopod shells and echinoid spines, bryozoans, coral debris (Fig. 7 j, k and l).

Description of microfacies

The microfacies is distinguished by the abundance of brachiopod and fossil debris. This grain-supported microfacies contains high amounts of skeletal debris. Brachiopod, coral and fossil debris (40%) with sizes up to 5 mm are the most important components. In some cases, crinoid and echinoid are observed (Fig. 7 j and Fig. 8 g). The shell beds formed by the accumulation of complete or broken shells are

characterized by medium bed grey limestone with an upward increasing trend in the proportion of fine particles.

Interpretation

Grainstone microfacies are interpreted to have shaped in a high-energy setting in the carbonate platform, in which skeletal elements were derived from adjacent facies. This is a characteristic of a setting situated above the FWFB in a barrier environment (Bover-Arnal et al. 2011). The presence of abundant skeletal components in some strata shoal is attributed to organisms such as reef. Moreover, their scarce lateral spreads may probably indicate a patch reef and deposited in a shallow open-marine shelf. As a result, small shell fragments could be easily moved by waves and currents. The above microfacies is comparable to SMF 12 of Wilson (1975) and RMF 28 of Flügel (2010).

11.4. Ooid grainstone microfacies

Field observations

This microfacies mainly take place in the medium to upper both sections. Fine to coarser-grained ooids-rich thin beds alternate within finer-grained muddy microfacies (tidal flat belt).

Description of microfacies

The major components of this facies are high abundance of ooids. Depositional texture is represented by grainstone (Fig. 8 b, c and d). Mainly ooids are radial and usually subspherical to subelongate, ranging in size from 0.1 to 0.7 mm, with an intermediate size of 0.5 mm. Bioclasts of this microfacies a little belong to crinoid, fragment fossil, and algae.

Interpretation

The grainy texture and sorting propose a high energy environment for this microfacies. The sediments would have been deposited in a barrier environment which separating the restricted shallow open-marine belt. This microfacies is explained as a barrier belt. Good grain arrangement and the deficiency of a vine matrix indicate the high energy status of the

shoal in this microfacies (Flügel 2010). Alike microfacies organization have been registered in the geological record (Sarg and Lehmann 1986). A similar facies type is described in north of the Kerman in Tabas block by Hashmie et al., (2016) Hossin abdi et al., 2015 and Wendt et al. (2002). The above microfacies is comparable to SMF 15 of Wilson (1975) and RMF 29 of Flügel (2010).

11.5. Bioclastic intraclastic grainstone microfacies

Field observations

This microfacies be composed of medium to thick-bedded dark grey beds containing brachiopod, intraclasts and fossil debris as major allochems.

Description of microfacies

Bioclast are the control ingredient (60%) and are smoothly scatter within the sparitic cement (Fig. 8 e). These bioclast be composed of different component such as coral, bryozoan, fragment brachiopods, crinoid and green algae. Intraclasts are often rounded. Some interclast are mentally uniform and composed of micrites, while others show interior compounds such as fossil debris (Fig. 8 e).

Interpretation

The abundant occurrence of skeletal ingredients shows that this microfacies deposited in proximity of shallow open-marine (Reolid et al. 2007 and Geel 2000). Grainstone texture, round intraclast and well-sorted components are indicators of high energy environment (Flügel 2010). Most of the intraclast are subangular to angular and some intraclasts are in the interior homogeneous. Such high energy deposits are typically collaborated with barrier and bioclast barrier (Flügel 2010). Such high-energy sediments are usually connected with bioclast barrier near or seaward (Wilson 1975; Flügel 2010). The above microfacies is able to be compared to SMF 13 of Wilson (1975) and RMF 27 of Flügel (2010).

11.6. Bioclastic grainstone microfacies

Field observations

This microfacies above contains of medium to thick-bedded grey beds. The main distinctive of this facies is the maximum variety of fossil in grain- uphold textures in the field.

Description of microfacies

Brachiopods and bivalve's debris, bryozoans, echinoids, gastropods, and algae are also present. The presence of biota and grain-supported texture in sparit cement and the absence of micritic matrix indicate a high energy state. Also, dolomitic and hematic are observed in these facies (Figs.8 g).

Interpretation

This microfacies is interpreted as a barrier belt above the fair climate wave base located at the edge of the platform, segregating the shallow open-marine belt from the restricted marine belt. The grain-supported texture, along with the large number of fossils, coral particles, and algae, suggests that the current medium to low-energy environment has occurred (Fournier et al. 2004). According to Flügel (2010), this is microfacies shared in shallow shelf interiors be composed of protect shallow-marine belt. According to Flügel (2010), this microfacies occurs in the interior of shallow shelf consisting of shallow marine environments protected by moderate water circulation. This microfacies is explained as a leeward barrier environment. Microfacies above is comparable to SMF 12 of Wilson (1975) and RMF 26 of Flügel (2010).

11.7. Bioclastic packstone/wackestone microfacies

Field observations

This microfacies be composed of light gray medium-bedded fine to coarse-grained bioclastic packstone/wackestone of sub-rounded to rounded ooids and bioclast with loose packing.

Description of microfacies

Fragment crinoid, coral and bryozoan are controlling components in this microfacies and other bioclasts are scarce (Fig.8 h and i).

Interpretation

The presence of healthy and well-preserved fossils shows a comparatively calm water environment with a steady bed and low sedimentation rate. Essence of skeletal debris of stenohaline skeletons which is mainly dependent of salinity and textural characteristics were formed on shallow open-marine area (Holcova and Zagorsek 2008). This interpretation is beared by the stratigraphic position and plentifulness of typical open marine skeletal fauna. This interpretation can be identified by the stratigraphic position and the presence of open marine skeletal animals including fossil debris and echinoids. The high difference of fossil and micritic matrix in microfacies point to moderate energy in a shallow open marine belt. This microfacies is able to be compared to SMF 10 of Wilson (1975) and RMF 7 of Flügel (2010).

12. Paleoenvironmental model and comparison with other depositional models

Paleoenvironmental and paleontologists have a vested interest in understanding how organisms conform to environmental change. During the Devonian, shallow-marine carbonate depositional systems occurred across the world, with supported reef development (Kiessling 2006 and Wright 1992). Microfacies and organic facies make it possible to identify different depositional settings. Figures 4 and 5 show the ranges of the facies associations in our section. Based on conversed petro/microfacies and sedimentary analysis cooperatively with lithology broadcast and progressive shallowing tendency from the basin into the shallow shelf is proposed for the deposition of this formation at the studied region (Fig. 9). The lack of any marginal reef evolution, attendance of clastic pertofacies, no evidence of resedimentation and the existence of high energy facies is compatible with the Bahram Formation which is deposited in a carbonate-siliciclastic shelf (Figs. 4, 5).

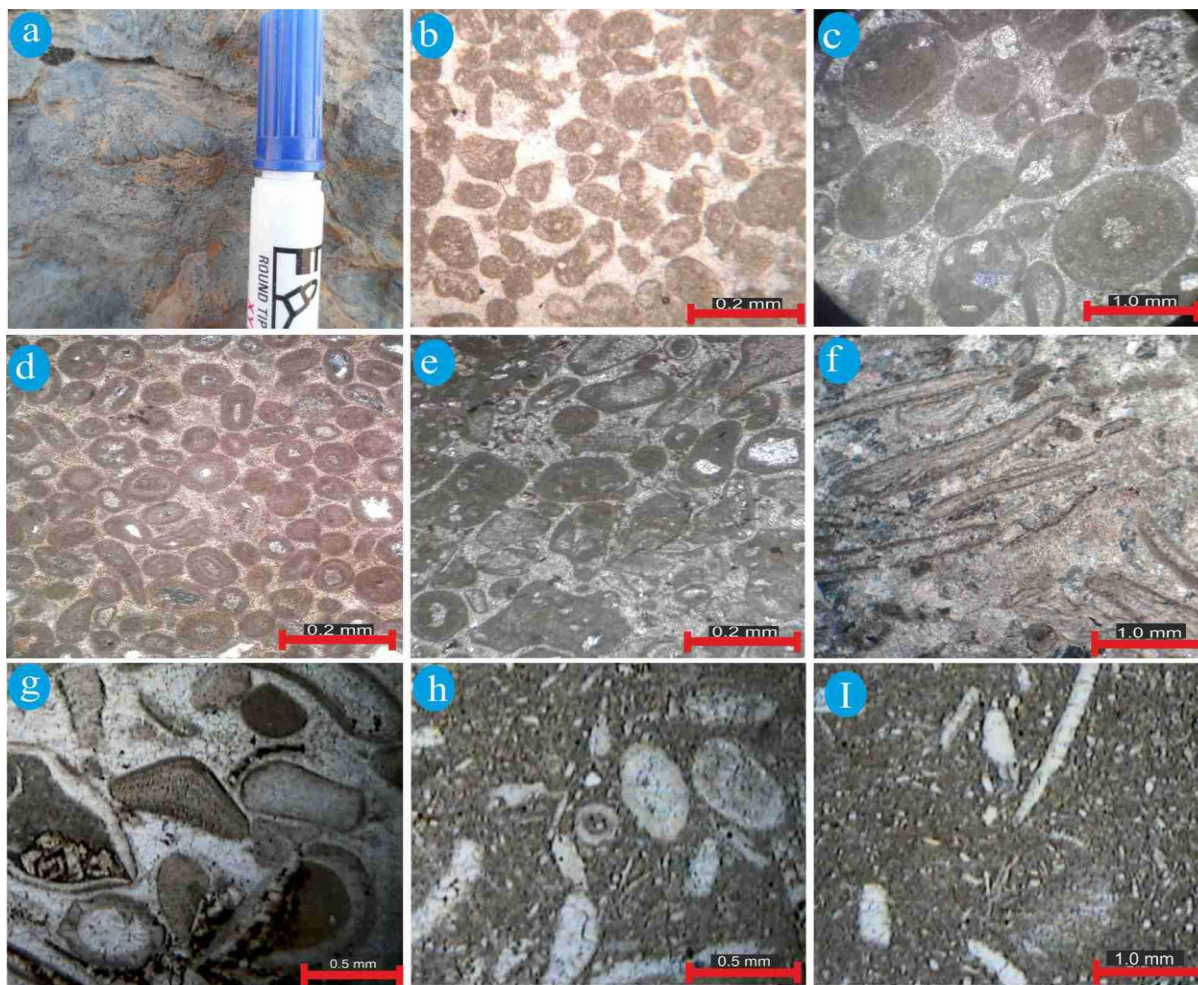


Fig. 8. (a) Gastropods and debris fossil in limestone bed. (b) Ooid grainstone microfacies Sar-e-Ashk section. (c and d) Ooid grainstone microfacies in Shaftalugaltan section. (e and f) Bioclastic intraclast grainstone microfacies. (g) Bioclast grainstone microfacies. (h and i) Bioclastic packstone/wackestone microfacies. All photos are under XPL light.

Based on these studied facies, paleo-environment and sea level changes is recommended for deposition of the Bahram Formation in this studied region. Wendt et al. (2002 and 2005) introduced the occurrence of typical Devonian platform deposits in this area, similar to those on the CEIM, is noteworthy. The width of the facies is further achieved by a joining of depth slopes and nutrients in a perfect transect from the inner shelf to the middle shelf (Fig. 3). Shore facies include shore face and offshore sediment environments, under the influence of permanent immersion (more in Sar-e-Ashk section). Stressed conditions in Shaftalugaltan section, regeneration is returned by the fabric of fenestrate and the absence of bioclasts. The attendance of mud-supported textures and the obvious lack of current and wave structures indicate the presence of a low-energy below the storm surge in the lagoon environment (Burchette and Wright 1992). In-

place, the grainstone facies are widespread in the barrier of the rimmed shelf and these conditions are typical for high energy environments in both sections. The micritic matrix in both section and the high diversity of fossil refers to moderate to low energy in a shallow open-marine environment. Marine regression resulted from the Frasnian-Famennian caused the deposition of the Bahram Formation, which is an indication of shallowing the basin as a result of this orogeny or the padeha Formation and unit1, 2 in Bahram Formation reflects the first (non-marine) onlap in response to thermo-tectonic subsidence in the aftermath of Frasnian-Famennian (e.g. Wendt et al. 2002, and 2005) (Fig. 9a). Thermo-tectonic subsidence after the Famennian phase added to the depth of the deposited basin and the inclination of continental fabric in marine facies, but the deposits basin was unstable. This formation has been formed in the carbonate

-clastic environment, which occasionally underwent fluctuations due to orogenic movements, retrograding toward the southwest and northeast in Central Iran. Bahram Formation in the south of Central Iran (Sar-e-Ashk section) has deposited in a shore to shallow open-marine and in an environment shallower than the north of Central Iran (Shaftalugaltan section) (Fig. 9). There is considerable document for the gradual resumption and severity of tectonic forces and the gradual increase of chemical sediments in shallow depressions leading to Devonian succession deposition. Facies in Formation are showing of sedimentation in an instable basin characterized by very variable facies. Terrigenous deposits with characterize such as cross-bedding and ripple marks in organization with mature lithofacies and fine-crystalline dolomite show that have deposited in a shore or tidal flat belt (Siddiqui et al. 2017). The reef builders are partly toppled and concentrated to coquinas, apparently by storm events in south Central Iran (Sar-e-Ashk section). Presences are all evidence of deposition in a wide carbonate-elastic shelf. The During the Frasnian in Shaftalugaltan section, carbonate-dominated Formation of changeable shallow to moderately deep marine have been deposited in this section. This drowning is slightly younger than in Shaftalugaltan section, but the general trend of a major comparative sea-level rise while the Frasnian is also evident from Torbat-e-Jam area (Wendt et al. 2005). The skeletal and non-skeletal components match well those known from modern shallow- and fresh-water carbonate systems, suggesting open shelf settings. Generally, the basal tectonic unconformity is connected to the Devonian tectonic event, indicating a considerable palaeo-relief that has been leveled by the basal Padeha Formation. In their Unit3 in Sar-e-Ashk section, intercalated marginal marine indicate shortcuting of restricted sea environments.

13. Sequence stratigraphy

Stratigraphic analysis method for sea level changes used in this research is based on the model delineated by Emery and Myers (1996) and Catuneanu, (2006 and 2019) and Catuneanu et al. (2009) who reasonable three standard systems of 3rd-order (Vail et al. 1977)

(LST, TST, HST). Cyclicity of the Shaftalugaltan (Bahram Formation) Sedimentary layers are still relatively poorly known, but this study suggests that this replacement could benefit from a stratigraphic sequence order, which would make it possible to evaluate the main strata controls using relative sea level variation locally. (Figures 4, 5, 9 and 10).

13.1. Sequence 1

This sequence comprises the Lower Bahram Formation and the depositional this sequence formed during the lower Frasnian. This sequence consists of shallow inner to mid-shelf facies with similar thicknesses ranging from 87m and it overlies basinal siliciclastic of the Padeha Formation with dolomite Sibzar (Figs. 4, 5 and 10). This sequence in other sectoins the south central Iran (CEIM) forms more thicknes layers. This sequence is of the megasequence (Kaskaskia Cycle) (Ogg et al., 2004) and deposited during Frasnian time in mixed clastic/carbonate platform. This sequence formed LST, TST and HST that are described below: The lower boundary of Bahram Formation is marked at the top of the Padeha Formation with dolomite sibzar in two sections (Fig. 10 a and b). Therefore, an irregularity is formed between Padeha and Sibzar Formations and it is analyzed as the boundary of type 1 sequence at the base of sequence 1. The thickness of lowstand system tract (LST) is about 26 m and consists of dolomite Shotori Formatoin, dolomitic mudstone and bioclastic intraclast grainstone. As this system tract deposited shallow water and in tidal flat and barrier sedimentary environment. The thickness of LST at Central-East-Iran Microplate is more than Shaftalugaltan section that can be related LST deposition. LST sediments in all sections often include carbonate silicate facies and sand grains in the facies, which reflect the influx of sediments in these sections. The onset of interaclast with fossiliferous limestone (Bioclast interclast grainstone micfacies) depict the TS and the start of the TST. Thickness of TST facies ranges from 20 m and it is characterized by increasing the carbonate sequence to a horizontal thickness of the flat tide and shoal from toward open marine facies.

The mfs was determined by the presence of bioclastic packstone/grinestone microfacies that are very rich in fossil debris. After the mfs stage, there was a progressive progradation of bioclast-rich facies (brachiopods, coral, bryozoan, fragment fossil and...) and the proximal facies, and this shallow to the top unit depict the HST. The thickness of high stand system tract (HST) microfacies ranges 43m and shallowest inner shelf, tidal flat toward restricted lagoon microfacies deposited. The topmost boundary of this sequence with some uncertainty is type 2 and is positioned at the top of quartz wacke microfacies (Fig. 9). The shallow to the top course from coastal is showing of a progradational stacking pattern in HST (Kwon et al. 2006).

13.2. Sequence 2

This sequence higher thickness of carbonates productivity during shelf shallowing and deposition of inner-shelf (Fig8 and 9). This sequence also consists of TST and HST. The thickness of sequence2 decreases with a gradual trend from Sar-e-Ashk section to Shaftalugaltan section. The Lower boundary of sequence2, based on subordinate shore facies and no proof of denouncement, is apparently SB2 in this section. Due to tumble of sea level and epeirogenesis, the upper boundary of sequence2 is type 1 (SB1) and can be significant in the light grey horizon of sandstone in top Bahram Formation. This sequence in this section is coherent with sequence 2 in elsewhere (other sections) in Central Iran (CEIM). Due to erosion processes and lack accommodation, LST is not preserved and TST sediments directly cover the sequence boundary (SB and TS) (Zecchin and Catuneanu 2013). LST is not higher than SB1, usually due to the erosion cycle and possibly no sedimentation in this area. Hence TS is located at the top of the sequence boundary. The thickness of TST ranges between 18 m and the main facies are bioclastic packstone/wackestone and with thin interbeds of bioclast grainstone microfacies that could be created in the inter-tidal environment (Barrier). The maximum flooding surface (MFS) transgressive systems tract (TST) deposited is marked by dolomitic lime mudstone and interpreted a composite tidal flat toward shore

and separates TST from HST. Following TST, HST aggradational with slight progradation is combined of alternation of grey shale form and limestone that were formed in shoal belt. Above TST, dolomitic mudstone and Sandy dolomitic lime mudstone formed in the near-coast setting during HST. These deposits often formed in tidal flat toward offshore setting, therefore recognized sequence boundary (SB1). HST mirror an aggradational retrogradation of sandy dolomite and limestone with interlayer of shale makes up. These sequence were deposited when the accommodation equal to sediment supply. The above sediments settle when the accommodation is identical to the sediment supply.

13.3. Sequence 3

The upper boundary is overlying gray dolomite of Shotori Formation in Shaftalugaltan section and Jamal Formation in Sar-e-Ashk section (Fig10 c). This boundary is steadfast with the regression of shore line that is pursue continental sedimentation of the Jamal and Shotori formations. Sequence3 was not formed in some sections because of probably not depositional and fall of sea level region that led the upper Formation to be bare and corroded and tectonically driven heterogeneous subsidence (Fig11). These outcrops overlay bioclast-rich limestone of the bioclast interacast grainstone microfacies in barrier belt. At some section, this sequence is not existing (Fig.11b) and some uncertainty, is located at uppermost strata of the Bahram Formation. The rapid fall of the comparative sea level has caused the formation of a composite sequence boundary (TS SB type 2) at the base of TST sediments (Catuneanu et al., 2005). The sudden fall of the comparatively sea level forms the mixed sequence boundary (TS and SB) at the base of TST (Catuneanu et al., 2005). Sequence3 is 62 m (Shaftalugaltan section) and 42 m (Sar-e-Ashk section) thick whose facies organization can be grouped into TST and HST. MFS has been identified with fossil-rich marine facies that separate TST from HST. Likely an ooid bioclast grainstone with superabundant fossil debris cover the MFS. These sediments are interpreted as early HST, whose sediments are combined shoal facies. Inter-bedded shoal facies deposits with

alternative of limestone with fossil debris show late HST deposits. The late HST exhibit a tendency to add to sedimentation, mention a filling of the accommodation. The boundary among sequence 3 and Shotori and Jamal

formations is placed (Figs. 11 a and b) where this sequence is increasing sediment supply. A long period of sea situation, indicating a stable state between accommodation and the aggradational stacking pattern.

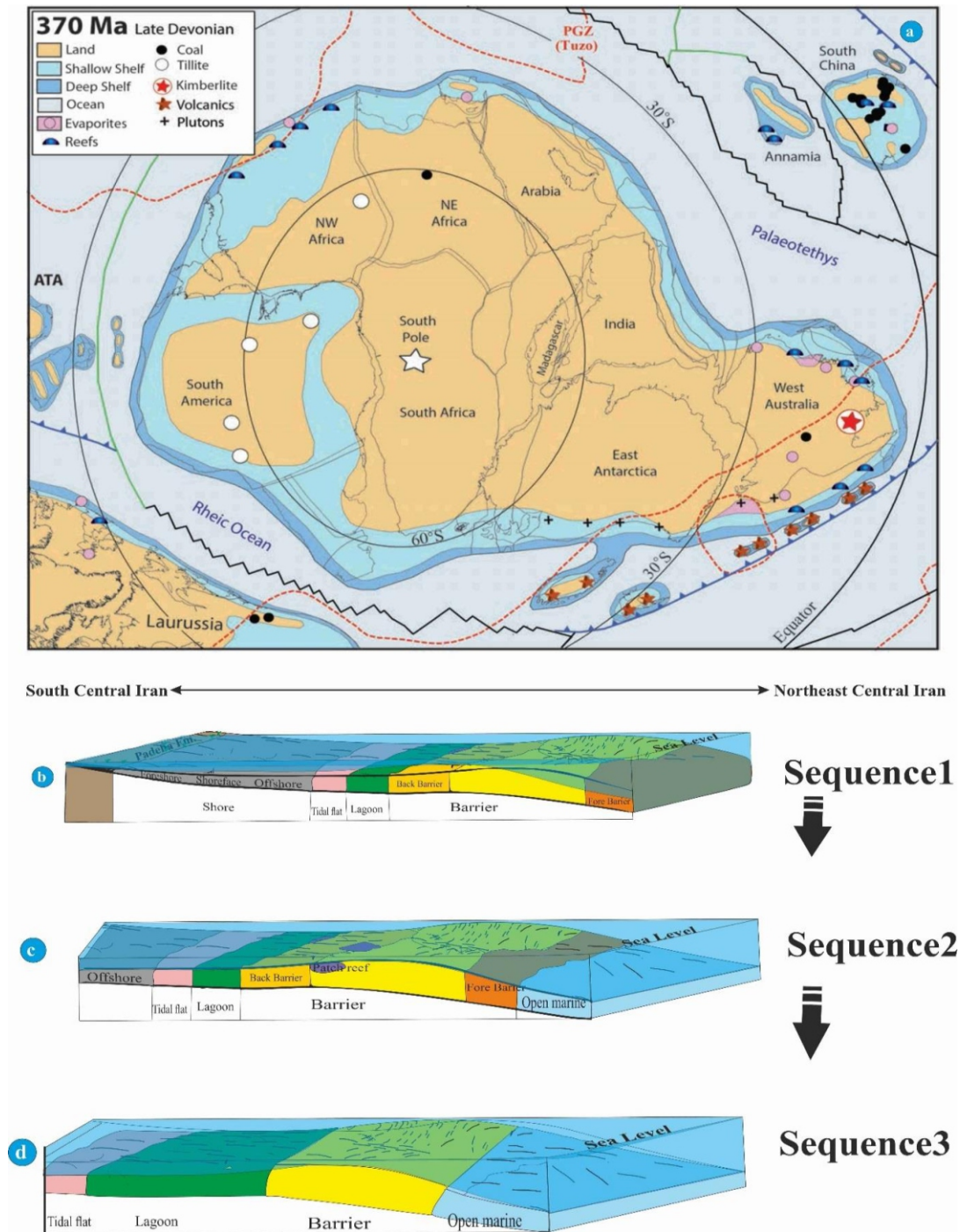


Fig. 9. (a) Paleo-tectonic, paleogeographic and lithology map of the north Gondwana land during the Frasnian and central Iran plates during the late Devonian (modified from Torsvik and Cocks 2013). (b) Schematic depositional models of the Bahram Formation during the Lower Frasnian and sequence No1. (c) Middle Frasnian and sequence No 2. (d) Upper Frasnian and sequence No 3. These local depositional models show a systematic progradation from SW to NE.

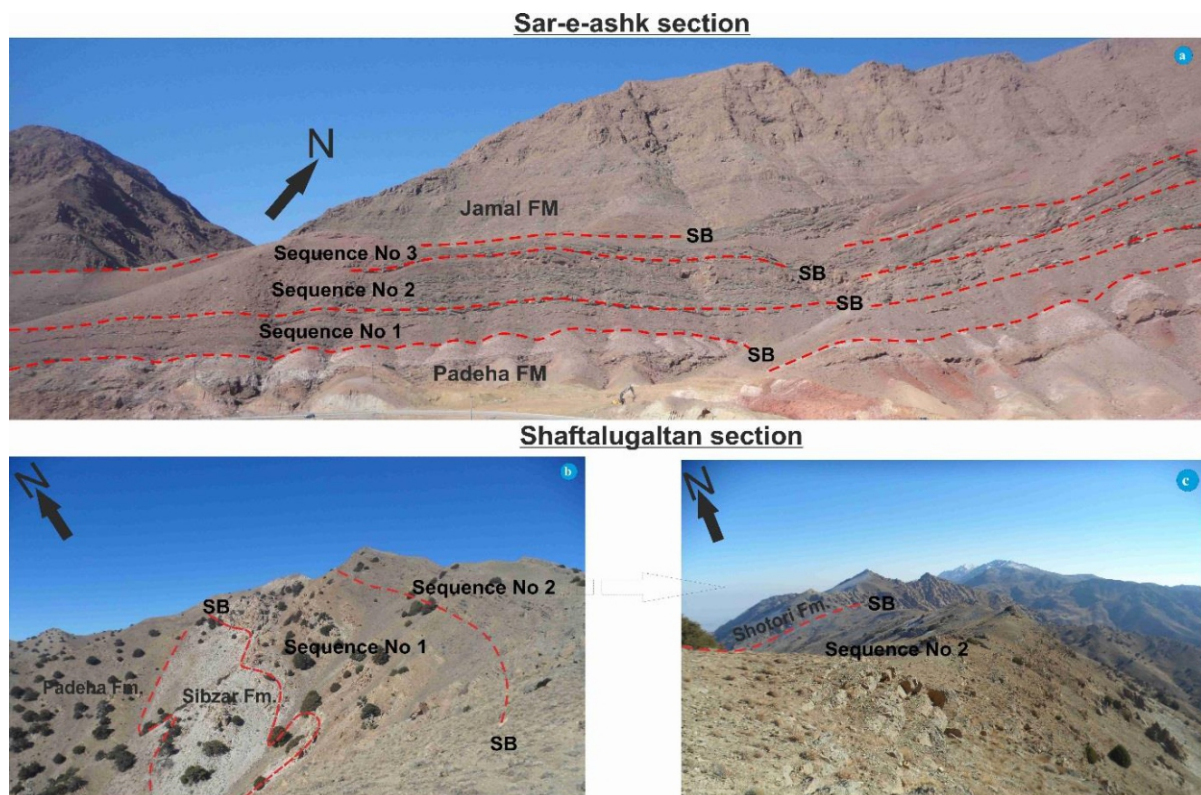


Fig. 10. (a) Field aspects of key outcrops of the Bahram Formation in Sar-e-Ashk section (b) Outcrop photograph of the studied section at the Shaftalugaltan section and panoramic view in field photographs showing depositional sequences and lower (c) upper boundaries of the Bahram Formation in study area. Abbreviation: SQ: Depositional Sequences.

14. Paleo environment correlations

The sequence of investigated Bahram Formation is a part of the transgressive–regressive megacycles Kaskaskia, which comprises the Devonian (Oog et al. 2004) (Fig11 b). This megacycle is characterized by tectonic instability and is increased subsidence rates, in contrast to the widespread uniform facies and thickness development during the Devonian (Hshmie et al. 2016). A relative sea-level highstand is inferred by the supremacy of repetitive deep-basinal marls during the Lower Frasnian in the Sar-e-Ashk section in deep basinal carbonate platform parts and in middle platform part at Shaftalugaltan section. The thickness of this sequence at Central-East-Iran Microplate is more than Shaftalugaltan section. The replace from a shallow-marine shelf to deep marine settings suggests a famous modification in depositional style; thus, the top surface of Bahram Formation depict a immersing unconformity. The sedimentary basin in the studied area has existed between the Kavir fault to the south and the Nayband fault to the east and Nain fault to the west in Sar-e-Ashk

section (Fig. 1). These data and observations provide information on how to limit the tectonic evolution of the study area. The correlation between sea level change and the main facies of the studied region in northern central Iran shows a deeper effect. Generally, the high ratio of shore, lagoonal, tidal-flat, barrier and shallow open-marine belt exhibit comparatively shallow-water situation. Due to facies changes, the trend of depth increase during deposition of Bahram Formation in Sar-e-Ashk section and other studied in south and north Tabas block is towards Shaftalugaltan section. To interpret observed relative sea-level changes, one needs to regard tectonic against eustatic controls. Deformation and uplift of the shallow marine of Central Iran during the Frasnian and Famennian are well registered by regression and connected facies changes (Wendt et al. 2002, 2005 and Hashmie et al. 2016). Changes in sea level in the studied area (sedimentary cycle) are almost inconsistent with global sea level changes due to sediment location and local tectonic activity. Whether the 3rd-order cycles of sequence 1 to sequence 3 given here are due to static or tectonic control,

so the answer is difficult. Even though tectonic events may affect the stratigraphic cycle at any time scale (Catuneanu 2019). Our study shows that, broadly speaking, we do not observe the thickness of sedimentary units or sudden facies changes, which expresses local or regional tectonic instability (Figure 11a). Therefore, most likely, it was a regional change in the Frasnian-Famenian rate of sea level rise has been the original control on fabric, paleoenvironment, and stratigraphic arrangement. Even if we are not able to design high-resolution biographical controls on our

departments, both Wendt et al. (2002), Hoseinabadi et al (2015), Hashmie et al. (2015 and 2016), Bahrami et al. (2015) and two sections represent three sea-level maxima throughou the Frasnian-Famennian. Therefore, it is concluded that eustatic rather than tectonic controls play a more important role in the formation of carbonate paleoenvironments in the study region. Local tectonic effects are relatively minor, possibly causing differential subsidence and differences in small-scale sea level fluctuations. (e.g., Hosseinabadi et al. (2015); Hashemi et al. 2015 and 2016).

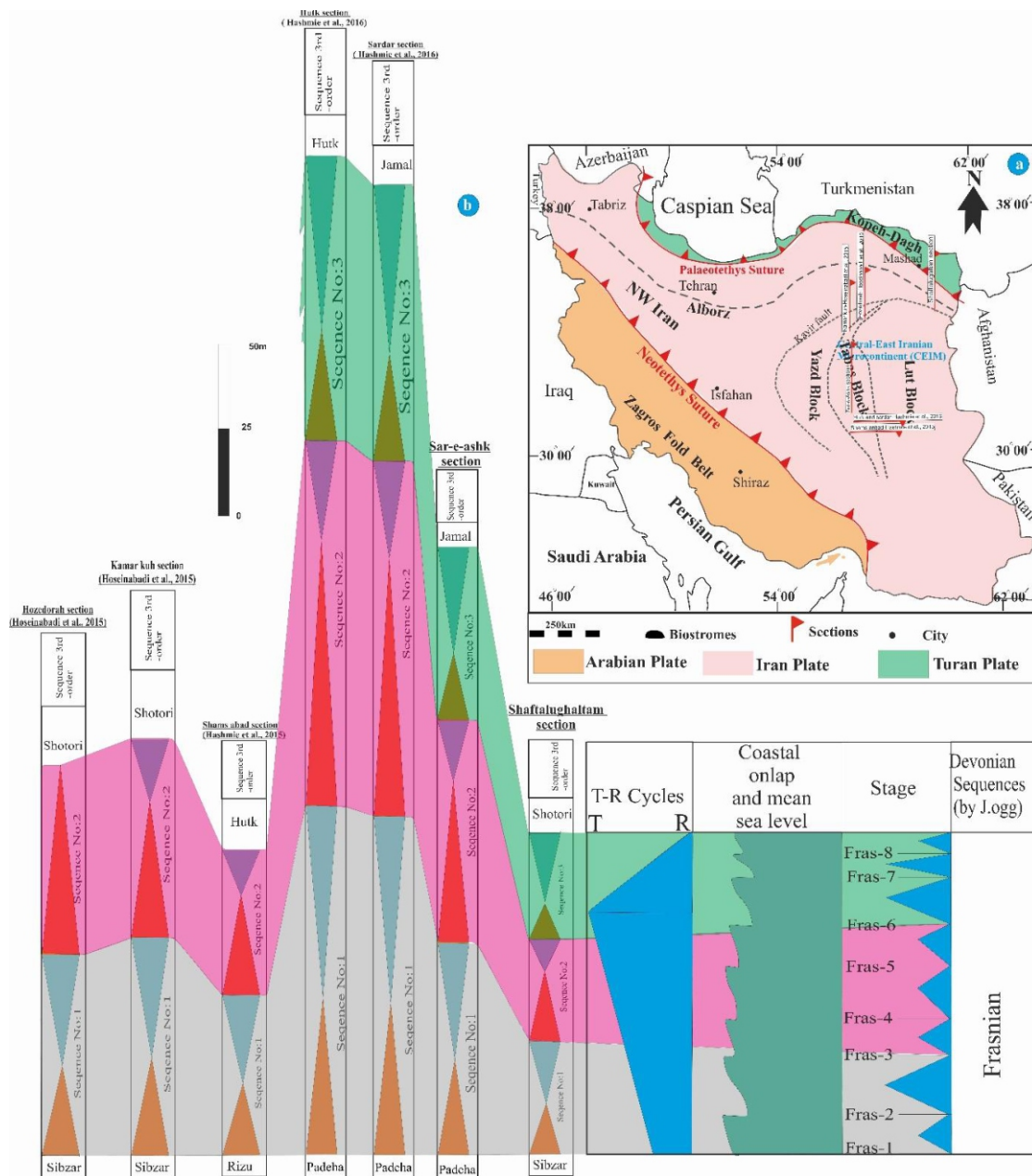


Fig. 11. (a) Location map of the studied area and correlation sections in Central Iran. (b) Sequences stratigraphy in the studied section of the Bahram Formation that correlated with other studied in Central Iran and sea level fluctuation in world.

15. Conclusions

The exposed Bahram Formation at the Shaftalugaltan and Sar-e-Ashk sections, of the Iran plate northeastward was studied on the basis of biostratigraphy, facies, paleoecological and sequence stratigraphy factors. Based on two zones *Umbella rotundata*, *Umbella shahrudensis* and *Umbella* sp., that Bahram Formation at the Shaftalugaltan section and conodonts in Sar-e-Ashk section is Frasnian in age. In this research stratigraphic sections, Bahram Formation upper the dolomite Sibzar and Padeha formations and underlies Shotori and Jamal formations and contains of thick medium to thick limestone, sandstone, sandy dololimestone and shale. The Bahram Formation shelf system of Frasnian age is excellently bare in three-dimensional outcrops showing a diversity of facies connected depositional geometries. The petrographical study of 149 thin sections of the Bahram Formation arrives to the identification of eleven facies, which were deposited in five microfacies belts of shallow marine, shoal, lagoon, tidal channel and shore. The comparison of the facies with the standard facies designated that the Bahram Formation is deposited in a mix carbonate-siliciclastic shelf including sub-environments of inner shelf and middle shelf. The Bahram Formation is represented by three and 3rd-order cyclic shallowing-upward carbonate sequences of siliciclastic deposits and carbonates. A gradual sea-level fall from Frasnian was presumably responsible for the decrease in the frequency of bioclast and abundance of clastic grain dominated. Sequences 1 are characterized by shore to shallow open marine facies Sequence 2 and 3 mainly consists of a shallow water environment in the base, followed by open marine to tidal flat facies. According to sequence stratigraphy three 3rd-order sequences and one regressive (LST) were distinguished with an overall systematic progradation from SW to NE in Iran plate. These progradations are evidenced in the Frasnian by major changes in facies. In order to better correlate the identified sequences with those predefined of the Bahram Formation in the Central east Iran micoplate that are chronologically well-known, we use their number instead of their name. Comparison of

the suggested succession with those reported in Iran plate and the regional comparative sea-level change curves correlate well with the global sea-level change.

Acknowledgments

We are very grateful to Dr. Mehdi Hadi and Dr. Ali Hashemi for their close help in this article. I thank the respected editors for their scientific opinions.

Author's Contribution

Ava Alizadeh: Assisted in library studies as well as lithological studies of the studied sequences and drawing a lithological column. Afshin Hashmie: proposed the main concept and involved in write up. Has collected all the field information and interpreted the paleoenvironment, sequence stratigraphic, final result, as well as various editions of the article. It has also drawn all the necessary images and coordination's. Neda Ghotbi: Has been involved in the interpretation of biostratigraphy.

References

- Aghanabati A., 2004. Geology of Iran. Geological Survey of Iran, Tehran, p 434 (in Persian).
- Alavi Naini M., Mossavi Khorzugh E, 1996. Geological Map of Iran, 1:100000 Series, Sheet 8160, Torbat-e- Jam, Geological Survey of Iran (GSI), and Tehran.
- Al-Juboury AI., AL-Hadidy A.H., 2009. Petrology and depositional evolution of the paleozoic rocks of Iraq. Marine and Petroleum Geology 26, 208-231.
- Bahrami A., Gholamalian H., Corradini C., Yazdi M., 2011. Upper Devonian conodont biostratigraphy of Shams Abad section, Kerman Province, Iran. Rivista Italiana di Paleontologia e Stratigraphia 117, 199-209.
- Bahrami A., Zamani F., Corradini C., Yazdi M., Ameri H., 2014. Late Devonian (Frasnian) conodonts from the Bahram Formation in the Sar-e-Ashk Section, Kerman Province, Central-East Iran Microplate. Bollettino della Società Paleontologica Italiana, 53 (3), 179-188.
- Blant G., 1978. Conclusion. In: Colloque

- Apports recents a la geologie du Gondwana, Lille, 1977, Annales de la Societe geologique du Nord, vol. 97, p. 414.
- Bozorgnia F., 1973. Paleozoic foraminiferal biostratigraphy of central and east Alborz Mountains, Iran. National Iranian Oil Company, Geological Laboratories Publication 4, 185p.
- Bozorgnia, F., 1964. Microfacies and microorganisms of Paleozoic through Tertiary sediments of some parts of Iran. With collaboration of S. Banafti. Publication of National Iranian Oil Company (Geological Laboratory) 158, 1–22.
- Burchette T.P., Wright V.P., 1992. Carbonate ramp depositional systems. *Sediment Geol* 79:3–57.
- Bykova E. V., 1955. Foraminifera and radiolarians from the Devonian of the Volga-Ural region and central Devonian areas and their use in stratigraphy, *Trudy Vsesoyuznogo Neftyanogo Nauchno-Issledovatel'skogo Geologo-Razvedochnogo Instituta (VNIGRI) Leningrad, n.s.*, 87: 5-141.
- Catuneanu O., 2006. Principles of Sequence Stratigraphy, first ed. Elsevier, Amsterdam, p. 375.
- Catuneanu O., 2019. Model-independent sequence stratigraphy. – *Earth-Science Reviews*, 188: 312–388.
- Catuneanu O., Abreu V., Bhattacharya J.P., Blum M.D., Dalrymple R.W., Eriksson P.G., Fielding C.R., Fisher W.L., Galloway W.E., Gibling M.R., Giles K.A., Holbrook J.M., Jordan R., Kendall C.G., Macurda B., Martinsen O.J., Miall A.D., Neal J.E., Nummedal D., Pomar L., Posa-mentier H.W., Pratt B.R., Sarg J.F., Shanley K.W., Steel R.J., Strasser A., Tucker M.E., Winker C., 2009. Towards the standardization of sequence stratigraphy. *Earth Sci. Rev.* 92, 1-33.
- Copper P., 2002. Reef development at the Frasnian-Famennian mass extinction boundary. *Palaeogeogr. Palaeoclimatol. Palaeoecol.* 181, 27-65.
- Dastanpour M., Bassett M., 1998. Palaeozoic sequences in Kerman region. In: Mawson, R., Talent, J.A., Wilson, G. (Eds.), UNESCO_IGCP Project 421, North Gondwana and Mid-Palaeozoic Bioevent/biogeography Patterns in Relation to Crustal Dynamics, Esfahan Meeting (17-20 December, 1998. Shahid Bahonar University, Kerman, Iran, p. 21. Abstract book.
- Dorrik A.V.S., 2010. Sedimentary Rocks in the Field: A colour guide, fifth ed. Manson Publishing Ltd, p. 320.
- Dunham R.J., 1962. Classification of carbonate rocks according to depositional texture. In: Ham, W.E. (Ed.), Classification of Carbonate Rocks. American Association of Petroleum Geologists Memoir 1, pp. 108-121.
- Eftekhari Nezhad J., Alavi Naini M., Behruzi A., 1983. Geological Map of Iran, 1:100000 Series, Sheet 8060, Kariz Now, Geological Survey of Iran (GSI), Tehran.
- Embry A..F., 2009 Practical sequence stratigraphy. *Can. Soc. Petrol. Geol. Reservoir* 36, 1–6.
- Embry A.F., Klovan J.E., 1971. A late Devonian reef tract on Northeastern Banks Island, NWT. *Bulletin of Canadian Petroleum Geology* 19, 730-781.
- Emery D., Myers K., 1996. Sequence Stratigraphy. Blackwell, Oxford, p. 297.
- Flügel E., 2010. Microfacies of Carbonate Rocks, Analysis, Interpretation and Application. Springer-Verlag, Berlin, p. 976.
- Flügel H., Rüttner A., 1962. Vorbericht über paläontologisch-stratigraphische Untersuchungen im Paläozoikum von Ozbak-kuh (NE Iran). *Geologischen Bundesanstalt* 2, 146-150.
- Fournier F., Montaggioni L., Borgomano J., 2004. Paleoenvironments and high frequency cyclicity from Cenozoic South-East Asian shallow-water carbonates: a case study from the Oligo-Miocene buildups of Malampaya, Offshore Palawan, Philippines. *Marine and Petroleum Geology* 21, 1-21.
- Geel T., 2000. Recognition of stratigraphic sequences in carbonate platform and slope deposits: empirical models based on microfacies analysis of paleogene deposits in southeastern Spain. *Palaeogeogr. Palaeoclimatol. Palaeoecol.* 155:211–238.
- Ghavidel-syooki M., Mahdavian M., 2010. Palynostratigraphy of Devonian strata in Hutak area, northern Kerman Province.

- Stratigraphy and Sedimentology Researches 39, 19-32 (in Persian).
- Gholamalian H., 2003. Age implication of late Devonian conodonts from the Chahrisah area northeast of Esfahan, central Iran. *Courier Forschungsinstitut Senckenberg* 245, 201-207.
- Gholamalian H., 2007. Conodont biostratigraphy of the Frasnian-Famennian boundary in the Esfahan and Tabas areas, Central Iran. *Geological Quarterly* 51, 453-476.
- Gholamalian H., Ghorbani M., Sajadi S.H., 2009. Famennian conodonts from Kal-e-Sardar section, Eastern Tabas, Central Iran. *Rivista Italiana di Paleontologia e Stratigrafia* 115, 141-158.
- Gholamalian H., Kebriaei M.R., 2008. Late Devonian conodonts from the Hojedk section, Kerman Province, Southeastern Iran. *Rivista Italiana di Paleontologia e Stratigrafia* 114, 171-181.
- Gregg J.M., Shelton K.L., 1990. Dolomitization and dolomite neomorphism in the back reef facies of the Bonnetterre and Davies Formations (Cambrian), southeastern Missouri. *Journal of Sedimentary Petrology* 60, 549-562.
- Hashmie A., Rostamnejad A., Nikbakht F., Ghorbanie M., Rezaie P., Gholamalian H., 2015. Depositional environments and sequence stratigraphy of the Bahram Formation (middle-late Devonian) in north of Kerman, south-central Iran. *Geoscience Frontiers*, 1-14P.
- Holcova Z., Zagorsek K., 2008. Bryozoa, foraminifera and calcareous nannoplankton as environmental proxies of the bryozoan's event in the Middle Miocene of the Central Paratethys (Czech Republic). *Paleogeography, Paleoclimatology, Paleoecology* 267:216-234.
- Hoseinabadi M., Mahboubi A., Shabestari G. M., Motamed A., 2015. Depositional environment, diagenesis, and geochemistry of Devonian Bahram formation carbonates, Eastern Iran. *Arab J Geosci*, 2-25p.
- Husinec A., Sokac B., 2006. Early Cretaceous benthic associations' foraminifera and calcareous algae of a shallow tropical-water platform environment (Mljet Island, southern Croatia). *Cretaceous Research* 27, 418-441.
- Husseini M.I., 1991. Tectonic and depositional model of the Arabian and adjoining plates during the Silurian-Devonian. *American Association of Petroleum Geologists Bulletin* 75, 108-120.
- Khalifa M.A., 1982. Geological and Sedimentological Studies of West Beni Mazar Area, South El Fayium Province, Western Desert, Egypt. Ph.D. Thesis, Cairo University.
- Khalifa M.A., Morad S., 2015. Impact of depositional facies on the distribution of diagenetic alterations in the Devonian shoreface sandstone reservoirs, Southern Ghadamis Basin, Libya. *Sedimentary Geology* 329, 62-80p.
- Khosravi Z. M., Hosseini-Nezhad SM, 2014. Sequence Stratigraphy of Padeha and Bahram Formations in Baghin Section (West of Kerman) based on Lithofacies and Conodontfacies, *Scientific Quarterly Journal, Geosciences*, Vol. 23, No. 92. (In Persian).
- Kiessling W., 2006. Towards an unbiased estimate of fluctuations in reef abundance and volume during the Phanerozoic. *Biogeosciences* 3, 15-27.
- Kwon Y.K., Chough SK., Choi D.K., Lee D.J., 2006. Sequence stratigraphy of the Taebeak group (Cambrian-Ordovician) Mid-east Korea. *Sedimentary Geology* 192, 19-55.
- Lacombe O., Mouthereau F., Kargar S., and Meyer B., 2006. Late Cenozoic and modern stress fields in the western Fars (Iran): Implications for the tectonic and kinematic evolution of central Zagros. *Tectonophysics*, 25, TC1003, doi: 10.1029/2005TC001831.
- Madler K., 1957 a. Charophyten, In: Freund, H., *Handbuch der Mikroskopie in der Technik*. Frankfurt am Main, Umschau Verlag, 3(3): 279-286.
- Madler K., 1957b. Fossil charophytes, their evolution, taxonomy and stratigraphy. *Journal of the Palaeontological Society of India*, 2: 2-47.
- Mahboubi A., Moussavi-Harami R., Lasemi Y., Brenner L.R., 2001. Sequence stratigraphy and sea level history of the Upper Paleocene strata in the Kopet-Dagh Basin, northeastern Iran. *AAPG*. 85:839-859.

- Miall A. D., 2006. *The Geology of Fluvial Deposits: Sedimentary Facies, Basin Analysis and Petroleum Geology*. – 582 pp.; Springer-Verlag.
- Mistiaen B., Brice D., Hubert B.L.M., Pinte E., 2015. Devonian palaeobiogeographic affinities of Afghanistan and surrounding areas (Iran, Pakistan), *Journal of Asian Earth Sciences*, 102–126.
- Morzadec P., Dastanpour M., Wright A.J., 2002. Asteropygine trilobites from the late Devonian of the Kerman region, Iran. *Alcheringa* 26, 143–149.
- Ogg J.G., Agterberg F.P., Gradstein F.M., 2004. The Devonian Period. In: Gradstein F., Ogg J., Smith A., editors. *A Geological Time Scale 2004*. Cambridge University Press.
- Pettijohn F.J., Potter P.E., Siever R., 1987. *Sand and Sandstone*, second ed. Springer, New York, p. 553.
- Ruttner A.W., Nabavi M.H., Hajian J., 1968. *Geology of the Shirgesht Area (Tabas Area, East Iran)*. Geological Survey of Iran, Reports 4, p. 133.
- Sarg J.F., Lehmann, 1986. Lower–Middle Guadalupian facies and stratigraphy, San Andres/Grayburg Formations, Permian basin, Guadalupe Mountains, New Mexico. In: Moore, G.E., Wilde, G.L. (Eds.), *Lower and Middle Guadalupian Facies, Stratigraphy and Reservoir Geometries, San Andres/Grayburg Formations New Mexico and Texas*. SEPM, Permian Basin Section Publication 86–95, pp. 1–8.
- Schlager W., 2005. Carbonate sedimentology and sequence stratigraphy. *SEPM Concepts in Sedimentology and Paleontology* 8 (200 pp.).
- Sengor A.M.C., 1990. A new model for the late Palaeozoic–Mesozoic tectonic evolution of Iran and implications for Oman. *Geochem Soc Spec Publ* 49:797–831.
- Sepehr M., and Cosgrove J.W., 2004. Structural framework of the Zagros Fold-Thrust Belt, Iran. *Mar. Pet. Geol.*, 21:829–843.
- Sharland P.R., Archer R., Casey D.M., Davies, R.B., Hall S.H., Hevard A.P., Horbury A.D., Simmons M.D., 2001. *Arabian Plate Sequence Stratigraphy*. GeoArabian, Special Publication 2, p. 270.
- Stewart Edgell H., 2003. Upper Devonian Charophyta of Western Australia, micropaleontology, vol. 49, No. 4, pp. 359–374.
- Stocklin J., Eftekhar-Nezhad J., Hushmand-Zadeh A., 1965. *Geology of the Shotori Range (Tabas Area, East Iran)*. Geological Survey of Iran, Reports 3, p. 69 (in Persian).
- Strasser A., Pittet B., Hillgartner H., Pasquier J.B., 1999. Depositional sequences in shallow carbonate-dominated sedimentary systems: concepts for a high-resolution analysis. *Sedimentary Geology* 128, 201–221.
- Tomasovych A., 2004. Microfacies and depositional environment of an Upper Triassic intra-platform carbonate basin: The Fatric Unit of West Carpathians (Slovakia). *Facies*. 50:77–105.
- Tucker M.E., Wright V.P., 1990. *Carbonate Sedimentology*. Blackwell Science, Oxford (482 pp.).
- Vahdati-Daneshmand F., Mosavvary F., Mahmudy Ghareei M.H., Ghasemi A., 1995 *Geological Map of Zarand*, 1-100,000 Series. Sheet 7351. *Geology Survey of Iran*, Tehran.
- Vail P.R., Mitchum Jr., R.M., Thompson S., 1977. Seismic stratigraphy and global changes of sea level, part four: global cycles of relative changes of sea level. In: Payton, C.E. (Ed.), *Seismic Stratigraphy Application to Hydrocarbon Exploration AAPG Memoir* 26, pp. 83–98.
- Walker R.G., 2006. Facies models revisited: Introduction. In: Posamentier, H.W., Walker, R.G. (Eds.), *Facies Models Revisited*. SEPM Special Publication 84, pp. 1–17.
- Wanas H.A., 2008. Cenomanian rocks in the Sinai Peninsula, Northeast Egypt: Facies analysis and sequence stratigraphy. *Journal African Earth Science* 52:125–138.
- Webster G.D., Maples C.G., Mawson R., Dastanpour M., 2003. A cladid-dominated lower Mississippian crinoid and conodont fauna from Kerman Province, Iran, and revision of the glossocrinids and rhenocrinids. *Journal of Paleontology* 77, 35. Lawrence, Kansas.

- Wendt J., Hayer J., Karimi-Bavandpour A., 1997. Stratigraphy and depositional environment of Devonian sediments in northeast and east-central Iran. *Neues Jahrbuch für Geologie und Paläontologie Abhandlungen* 206, 277-322.
- Wendt J., Kaufmann B., Belka Z., Farsan N., Karimu-Bavandpur A., 2002. Devonian/Lower Carboniferous stratigraphy, facies patterns and paleogeography of Iran, Part I. Southeastern Iran. *Acta Geologica Polonica* 52, 129-168.
- Wendt J., Kaufmann B., Belka Z., Farsan N., Karimu-Bavandpur A., 2005. Devonian/Lower Carboniferous stratigraphy, facies patterns and paleogeography of Iran Part II. Northern and central Iran. *Acta Geologica Polonica* 55, 31-97.
- Wilmsen M., Fürsich F.T., Seyed-Emami, K.M., Majidifard, R., Zamani-Pedram, M., 2010. Facies analysis of a large-scale jurassic shelf-lagoon: The Kamar-e-Mehdi formation of east-central Iran. *Facies* 56, 59-87.
- Wilson J.L., 1975. Carbonate Facies in Geologic History. Springer-Verlag, New York, p. 471.
- Wright V.P.A., 1992 revised classification of Limestones: *Sedimentary Geology*, v. 76, p. 177-185.
- Zecchin M., Catuneanu O., 2013. High-resolution sequence stratigraphy of clastic shelves I: units and bounding Surfaces. *Mar. Pet. Geol.* 39, 1-25.